photonics

MDPI

Article

A Novel Metaheuristic Approach for Solar Photovoltaic Parameter Extraction Using Manufacturer Data

Salwan Tajjour [1], Shyam Singh Chandel [1], Hasmat Malik [2,*], Majed A. Alotaibi [3] and Taha Selim Ustun [4]

[1] Solar Photovoltaic Research Group, Centre of Excellence in Energy Science and Technology, Shoolini University, Solan 173212, Himachal Pradesh, India
[2] Department of Electrical Power Engineering, Faculty of Electrical Engineering, University Technology Malaysia (UTM), Johor Bahru 81310, Malaysia
[3] Department of Electrical Engineering, College of Engineering, King Saud University, Riyadh 11421, Saudi Arabia
[4] Fukushima Renewable Energy Institute, AIST (FREA), National Institute of Advanced Industrial Science and Technology (AIST), Fukushima, Koriyama 9630298, Japan
* Correspondence: hasmat.malik@gmail.com

Abstract: Solar photovoltaic (PV) panel parameter estimation is vital to manage solar-based microgrid operations, for which several techniques have been developed. Solar cell modeling using metaheuristic algorithms is found to be one of the accurate techniques. However, it requires experimental datasets, which may not be available for most of the industrial modules. Therefore, this study proposed a new model to estimate the solar parameters for two types of PV panels using manufacturer datasheets only. In addition, two optimization techniques called particle swarm optimization (PSO) and genetic algorithm (GA) were also investigated for solving this problem. The predicted results showed that GA is more accurate than PSO, but PSO is faster. The new model was tested under different solar radiation conditions and found to be accurate under all conditions, with an error which varied between 7.6212×10^{-4} under standard testing conditions and 0.0032 at 200 W/m^2 solar radiation. Further comparison of the proposed method with other methods in the literature showed its capability to compete with other models despite not using experimental datasets. The study is of significance for the sustainable energy management of newly established commercial PV micro grids.

Keywords: photovoltaics; sustainable energy; sustainable development goals; microgrids; metaheuristic techniques

Citation: Tajjour, S.; Chandel, S.S.; Malik, H.; Alotaibi, M.A.; Ustun, T.S. A Novel Metaheuristic Approach for Solar Photovoltaic Parameter Extraction Using Manufacturer Data. *Photonics* **2022**, *9*, 858. https://doi.org/10.3390/photonics9110858

Received: 6 October 2022
Accepted: 9 November 2022
Published: 13 November 2022

1. Introduction

Solar technologies are the most efficient resources of energy and have been extensively utilized for power generation worldwide in the last decades. About 48TW of energy is available daily on earth, which can easily be harvested using photovoltaic (PV) panels to generate electricity [1]. However, before installing any solar plant, investors need to know the plant's performance and efficiency. The estimation of generated power from photovoltaic (PV) microgrids is important for energy management to balance generation as per demand in small townships/higher education institutions.

The main aim of this study was to develop a new model to predict power generation by roof top microgrids for reliable energy management using metaheuristic algorithms. Several techniques were used to estimate the power generation of photovoltaic microgrids. Solar cell modeling, in combination with metaheuristic algorithms, can effectively be used for accurate power generation extraction. A solar cell can be represented by single (SDM)-, double (DDM)-, or triple (TDM)-diode models with several parameters. The modeling accuracy is highly dependent on solar cell parameters. However, all these parameters are not provided by the manufacturing industry. Single-diode models (SDM) are usually used in the literature due to their simple structure and efficient identification [2]. Modeling

solar cells is vital for different applications, such as power generation estimation [3], maximum power point tracking [4], and degradation analysis [5]. Therefore, it is important to determine the modeling parameters accurately.

Analytical methods, which are used to solve this problem, depend significantly on some key points on the characteristic curves of the module such as the open circuit voltage and short circuit current. Thus, analytical methods are not very reliable and provide unsatisfactory results in most cases when many local minima points exist. Therefore, numerical methods are implemented to overcome this issue by considering all points. Some studies are carried out to solve this problem mathematically [6,7], which are also complex, slow, and based on assumptions. However, metaheuristic algorithms are mostly used due to their efficiency and accuracy. Zagrouba et al. [8] used a genetic algorithm (GA) to find the solar cell parameters values and the maximum power point (MPP) and found that GA is accurate and suitable with high efficiency. In refs. [9,10], the simulated annealing (SA) algorithm was compared with other techniques for SDM and DDM, and it was found to be much accurate and promising for two different experimental data. Mono-crystalline, multi-crystalline, and thin-film technologies were studied in ref. [11], wherein particle swarm optimization (PSO) with inverse barrier constraint was used to estimate the missing parameters of the modules. Another PSO algorithm was proposed in ref. [12] for physical systems' parameters extraction considering the Spectral Richness in the fast Fourier transform of the signals, which was found to reduce the variability of the estimates. A modified teaching-learning based optimization technique was used in ref. [13] to optimize the parameters of SDM and DDM for four different PV modules. Whippy Harris Hawks Optimization (WHHO) [14] is also used to find the optimal values of the solar models for three commercial modules under different conditions. Many other techniques are used in the literature for the same purpose, such as flexible PSO [15], Bacterial foraging algorithm [16], pattern search [17], Tree Growth-Based Optimization Algorithm [18], Coyote optimization algorithm [19], improved equilibrium optimizer [20], and enhanced ant lion optimizer [21]. A Firefly algorithm was proposed in ref. [22] for five, seven, and eight-parameter estimation for three types of modules, namely, R.T.C. France, flexible hydrogenated amorphous silicon a-Si:H, and a 36-cell module called PWP-201 and compared to other methods from the literature. For nine-parameter estimation, an Artificial Ecosystem-based Optimizer was proposed in ref. [23] and compared to other algorithms by testing on three commercial modules. An integration of the guaranteed convergence arithmetic optimization algorithm and Levenberg−Marquardt with the adaptive damping nonlinear parameter method was proposed for TDM in ref. [24] and was found to reduce the error to zero.

Machine learning techniques are data-driven techniques that require more datasets, tuning, and careful inputs selection [25]. They are also used for power generation and solar radiation forecasting and found to be effective to deal with big systems with a huge amount of uncertainty [26,27]. In these types of techniques, there is no need to define what circuit or parameters to use; rather, the algorithm will find the best relation between the inputs and outputs.

The performance of solar cells changes under different solar radiation and temperature conditions [28]. Therefore, the characteristics of any module are required to be drawn in order to analyze and estimate its performance. This can be completed by varying the voltage/current between certain values to obtain the I-V\P-V curves, but this requires experimental data, which require expensive setups and a lot of time, resources, and effort [29]. Therefore, this study proposed a new model to estimate the models' parameters using the manufacturing datasheets instead.

The novelty of this study is as follows:

- In the present study, a new model was proposed to estimate solar cell parameters using metaheuristic techniques requiring only manufacturer data instead of experimental data.

- The present model is more efficient as compared with other models in terms of accuracy, computational cost, and data required, whereas numerical methods are complex, slow, and based on assumptions. In addition, machine learning techniques require big datasets, more tuning, and careful input selection. Our model requires only three data points, which is even lesser than the requirements of solar cell modeling using experimental datasets.
- The three data points used from the manufacturer data sheet of PV modules were short circuit current I_{sc}, open circuit voltage V_{oc}, and the maximum power point current and voltage I_{mp}, V_{mp}.
- Two different types of solar modules, a single-cell module called R.T.C. France and a 36-cell module called PWP-201, were used for validation.
- A comparison of two metaheuristic algorithms, namely, genetic algorithm and particle swarm algorithm was presented.
- The results of the proposed model were further validated under varying solar irradiance conditions and compared to the same model using experimental datasets from the literature.

This paper is organized as follows In Section 2, the materials and methods are described; the results and discussion are exhibited in Section 3, and the conclusions and follow-up research are finally described in Section 4.

2. Materials and Methods

This study discussed the benefit of using PV module manufacturer datasheets for parameter estimation in order to model any given PV module. In this scenario, GA, PSO algorithms were used to solve the non-linear equation of a single-diode five parameters model for two types of modules: a single-cell module called R.T.C. France and a 36-cell module called PWP-201. Experimental datasets from the literature were collected to validate the proposed models, and a comparison of the measured data with the predicted ones was carried out. In addition, the algorithms used in this study were compared to other algorithms from the literature. Figure 1 depicts the methodology proposed in this study.

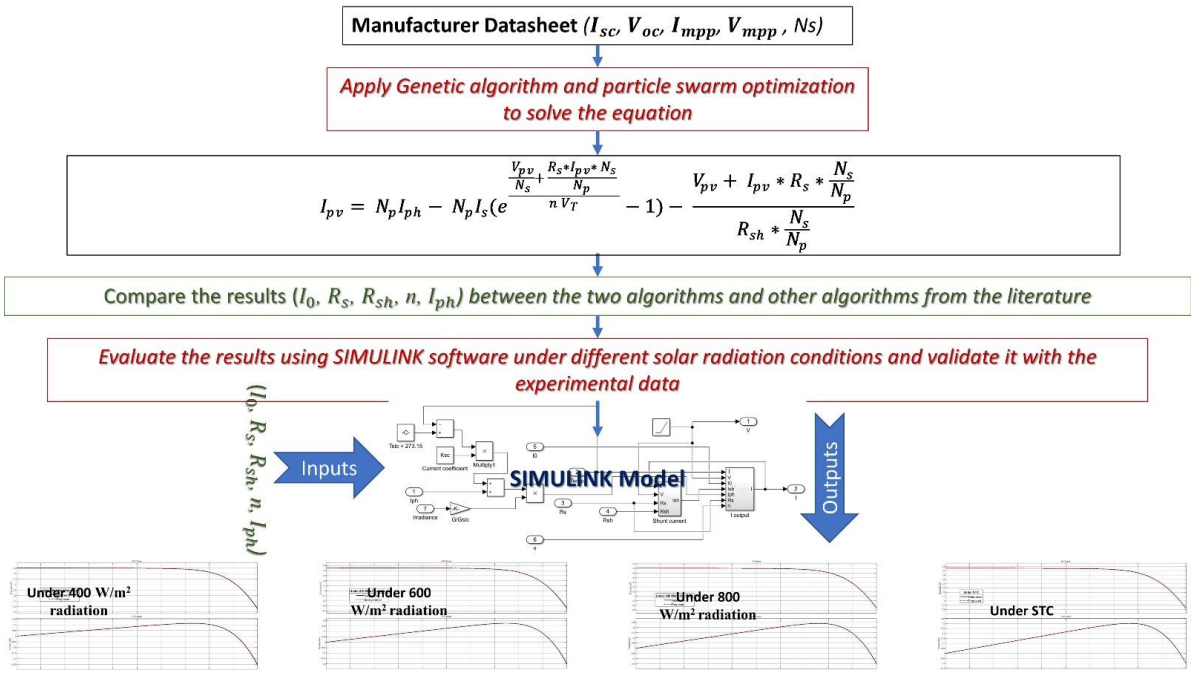

Figure 1. Methodology of the proposed study.

2.1. Single-Diode Five Parameters Model

Using SDM with five parameters is sufficient to model these types of modules [30]. The SDM contains a photocurrent source connected to one diode and one parallel resistor called a shunt resistor, *Rsh*, in addition to the R_s resistor, which was connected in series as demonstrated in Figure 2.

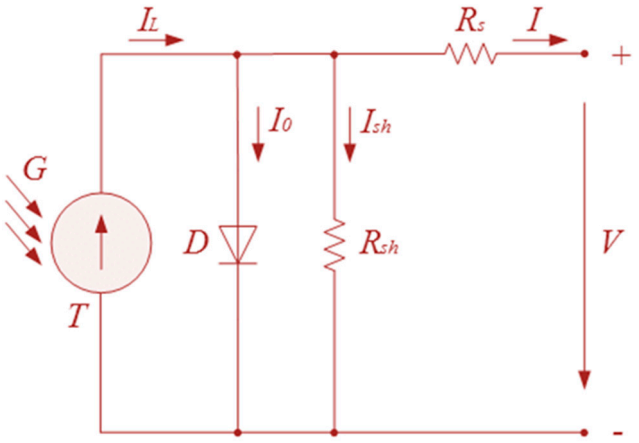

Figure 2. Schematic diagram of the single−diode circuit.

The current generated from the SDM was calculated using Equations (1) and (2) considering only one cell.

$$I_{pv} = I_{ph} - I_0 - \frac{V_{pv} + I_{pv} * R_s}{R_{sh}} \quad (1)$$

$$I_0 = I_s * (e^{\frac{V_{pv}+R_s*I_{pv}}{n\ V_T}} - 1) \quad (2)$$

where, I_{pv}, V_{pv} are the cell current and voltage, the reverse saturation current is I_s, n is the ideality factor, and the thermal voltage was calculated by the formula $V_T = \frac{kT}{q}$, where, T is the operating temperature of the cell, k is the Boltzmann constant, and q is the electron charge.

$$I_{ph} = \left[I_{phn} + K_{sc} * (T - T_{STC})\right] * \frac{G}{G_{STC}} \quad (3)$$

where I_{phn} is the photocurrent of the cell at the standard test conditions (which are usually equal to 25 °C and 1000 W/m^2), K_{sc} is the temperature coefficient of I_{sc}, T_{STC} is the reference temperature of the cell, G_{STC} is the reference irradiance, and G is the irradiance in W/m^2.

Solar cells were combined in series and parallel circuits in order to increase the generated power, since a single solar cell generates very low power. Therefore, the aforementioned equations can be modified to include the number of series cells N_s and parallel cells N_p used to form photovoltaic modules. The equation was derived from these equations as follows

$$I_{pv} = N_p I_{ph} - N_p I_s (e^{\frac{\frac{V_{pv}}{N_s} + \frac{R_s * I_{pv} * N_s}{N_p}}{n\ V_T}} - 1) - \frac{V_{pv} + I_{pv} * R_s * \frac{N_s}{N_p}}{R_{sh} * \frac{N_s}{N_p}} \quad (4)$$

In this study, the value of N_p was considered to be 1 as no cells were connected in parallel. Therefore, by considering Equations (1)–(4), the values of the 5 parameters (I_0, R_s, R_{sh}, n, I_{ph}) can be derived using optimization techniques and the proper objective function and data points.

2.2. Objective Function

Minimizing the difference between the predicted current and the current, which is actually measured, is the main objective of modeling. Root Mean Square Error (RMSE) is commonly used for evaluating such problems, and it can be formulated as in Equation (5):

$$RMSE = \sqrt{\frac{\sum_{i=1}^{N} \left(I_{i,actual} - I_{i,predict} \right)^2}{N}} \quad (5)$$

where the number of data points is N, the measured current is $I_{i,actual}$, and $I_{i,predict}$ is the predicted current using Equation (4).

2.3. Modeling Using MATLAB/Simulink

Simulink was used to model the circuit of single-diode models in order to assess the performance of the solar cells used in this study by drawing the I-V and P-V curves. MATLAB provides very useful tools to deal with such plots and compares them easily. The powerful features of Simulink make it easy to implement SDM and simulate the performance under different conditions. The entire block diagram of the model is given in Figure 3 and the sub-systems are given in Figures 4 and 5.

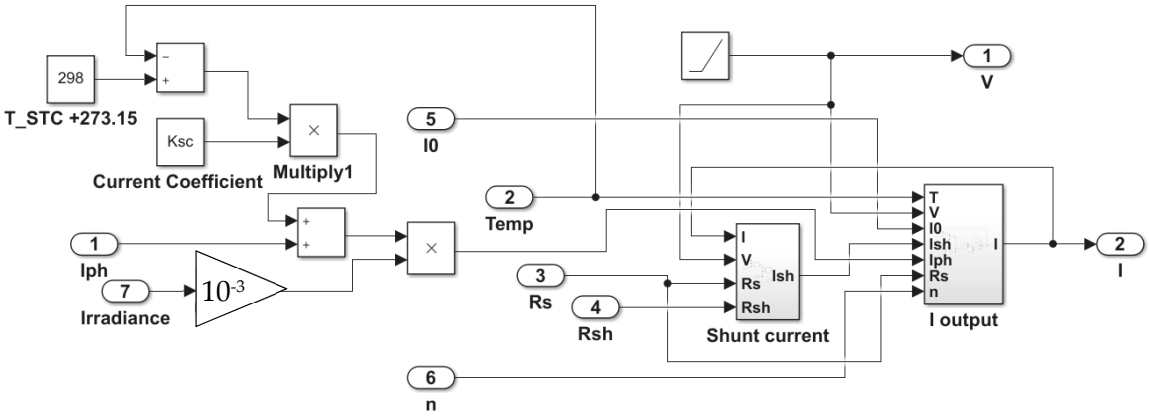

Figure 3. The entire module diagram.

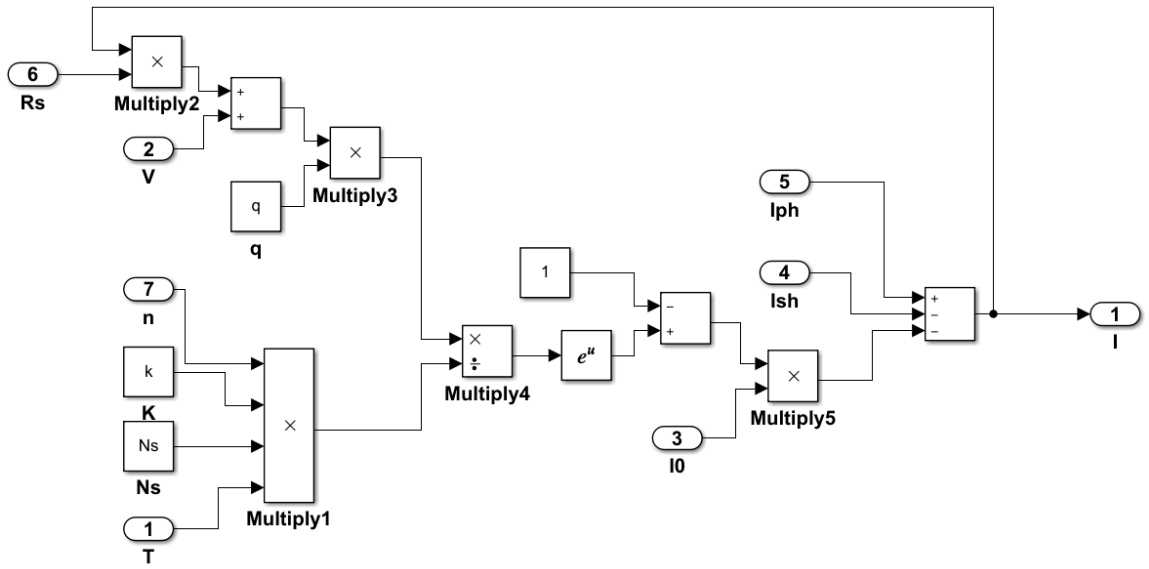

Figure 4. The output current diagram.

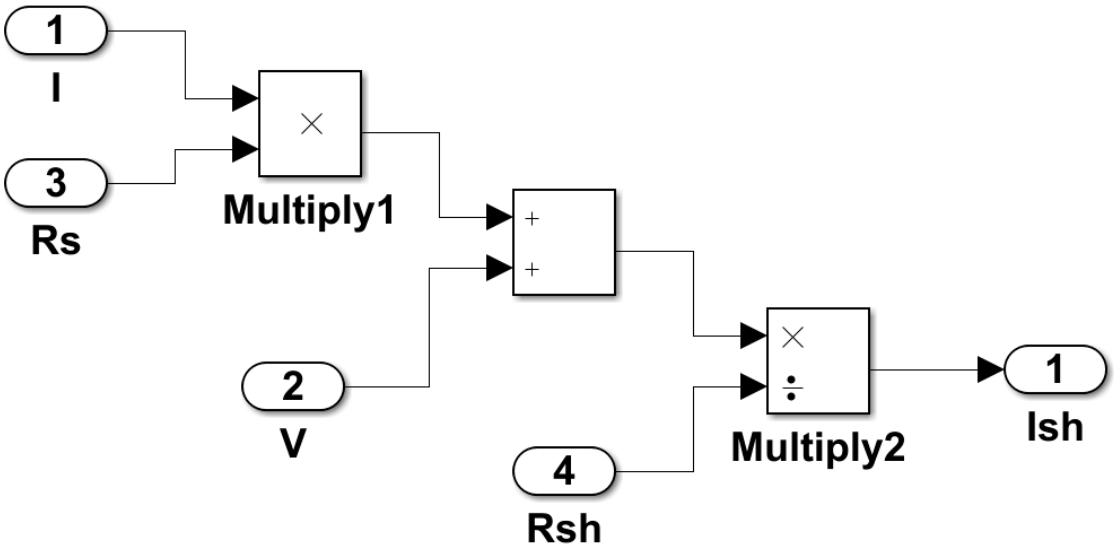

Figure 5. The shunt current diagram.

2.4. Genetic Algorithm

GA is a well-known optimization method belonging to the metaheuristic techniques. It imitates the rule "survival of the fittest" of natural evolution. GA can be implemented as shown in Figure 6 [31,32].

1. Selection of the main GA parameters, which are the size of the initial population, the number of maximum generations that can be reached, and the crossover and mutation probabilities.
2. Random initialization of the population. Generate matrix (X) representing (I_0, R_s, R_{sh}, n, I_{ph})
3. Calculation of the fitness using Equation (5) *f(X)*
4. Selection of the best population

$$Max\ (f\ (X))$$

5. Reproduce the selected individuals using variation operators considering the chosen probability, such as Crossover and Mutation, to generate new offsprings.

{If rand () < probability:
Operate Crossover (Equation (7))/Mutation (Equation (6));
Else:
Don't Change anything;
End}

$$Gaussian\ mutation\ x_i' = \sqrt{2}\,\sigma\,(\,b_i - a_i)\,erf^{-1}\,u_i' \tag{6}$$

$$\begin{cases} C_1 = \left(1 - \Upsilon\right) * P_1 + \Upsilon * P_2 \\ C_2 = \left(1 - \Upsilon\right) * P_2 + \Upsilon * P_1 \end{cases} \tag{7}$$

6. where, erf is the gauss error function, x_i is the offspring I, u_i is a random value between [0, 1], C_1 and C_2 are children of the parents P_1 and P_2, and Υ is calculated in (Equation (8)) by considering a, the constant which decides the range constraint of the offsprings and r, which is a random number

$$\Upsilon = (1 + 2a) * r \tag{8}$$

7. Compare the fitness of each individual and determine which ones will survive from the offsprings and the parents

Min (fitness (parents), fitness (offsprings))

8. Stop criteria identification

In this manner, GA proved to be more applicable for complex and real-world problems when multiple local minima occur. GA is adaptive to its environment, as this type of method is a platform which appears in a changing environment.

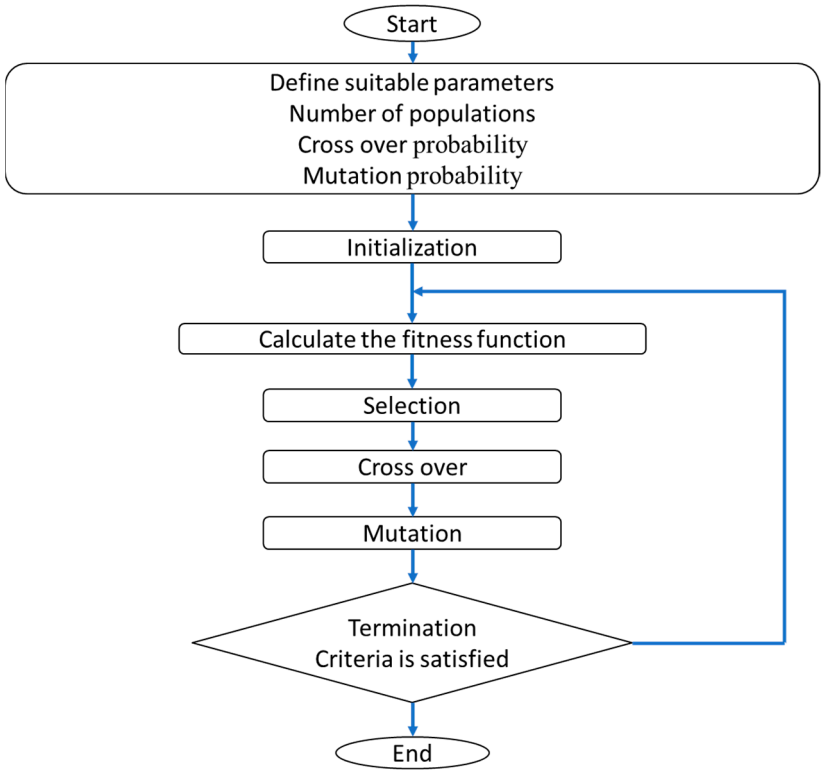

Figure 6. Genetic algorithm flow chart.

2.5. Particle Swarm Optimization

PSO is inspired by the swarm theory and the observation of the social behavior of animals. PSO can be implemented as follows (Figure 7) [33,34].

1. Choosing the main parameters, such as the number of particles, the velocity, and the positions;
2. Initialization of the population. Generate matrix (X) representing (I_0, R_s, R_{sh}, n, I_{ph});
3. Calculate the fitness of each particle using Equation (5);
4. Compare each particle with other particles based on the fitness and choose the best position to be the global point;
5. Update the particles' velocities using (Equation (9)) and send them to new positions:

$$V_i^{t+1} = W.V_i^t + C_1.U_1^t\left(P_{b_1}^t - P_i^t\right) + C_2.U_2^t\left(g_b^t - P_i^t\right) \quad (9)$$

6. Move the particles to new positions:

$$P_i^{t+1} = P_i^t + V_i^{t+1} \quad (10)$$

7. Check the stopping criteria.

Where, V_i^t is the velocity of the particle/agent i, W is the inertia weight, C_1 is the cognitive constant, U_1^t and U_2^t are random numbers, C_2 is the social constant, $P_{b_1}^t$ is personal best, and g_b^t is global best.

This makes PSO fast, computationally effective, and applicable for this kind of problem.

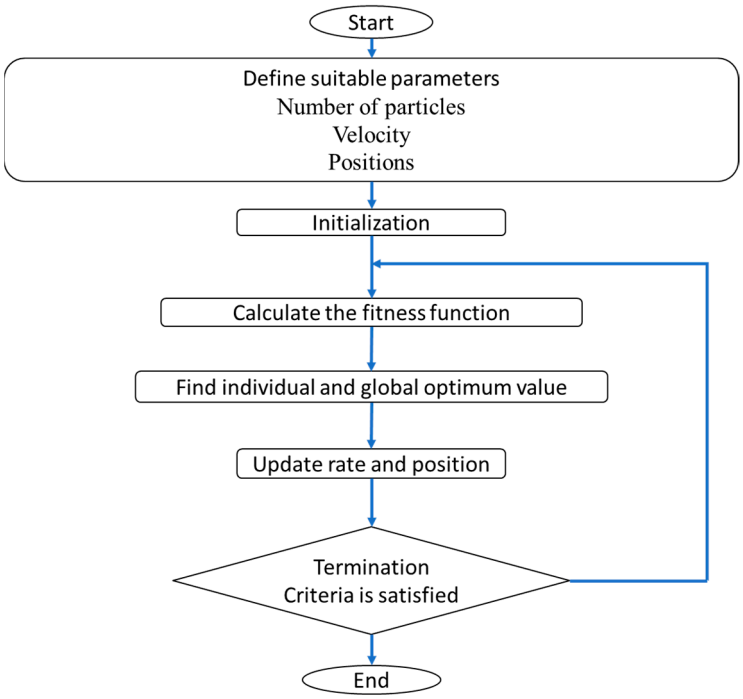

Figure 7. Particle swarm optimization algorithm.

2.6. The New Approach

In general, researchers take experimental measurements to feed the optimization techniques and find the parameters' optimal values. However, in some cases it is difficult to obtain such data, as it requires a set-up environment, particular tools, and time, and in some cases it is not worth it. Therefore, this study tried to solve this issue while maintaining a similar accuracy. This can be achieved by only taking the data available for all solar PV modules in the manufacturing datasheet.

Two PV panels were chosen in this study: R.T.C. France solar cell (which has a single cell) and PWP-201 PV module (which has 36 cells), to validate the proposed methodology results. The manufacturing values of the two panels are given in Table 1, which were taken under the standard condition of each module, and these values were used in the proposed methodology to find the five parameters with the help of Equations (1)–(4). Additionally, so were the experimental datasets which were taken from ref. [14].

Table 1. Manufacturing parameters for the R.T.C. France cell and PWP-201 module [14].

Variables	R.T.C. France Cell	PWP-201
I_{sc}, short circuit current	0.760	1.0317
V_{oc}, open circuit voltage	0.5728	16.778
I_{mp}, current at MPP	0.69119	0.912
V_{mp}, voltage at MPP	0.45	12.649
N_s, number of cells	1	36

PSO and GA were used in this study, as these algorithms are mature enough and well-studied in the literature where their efficiency to solve non-linear problems has been proven in various domains. Moreover, there are many stable and open-source libraries available

for both of them. In this study, MATLAB libraries were used for the implementation of these algorithms.

Both PSO and GA algorithms were used for parameter optimization using Equation (4) and the objective function given in Equation (5). The upper and lower limits of the parameters given in Table 2 for each PV panel were taken as suggested in refs. [14,35–41] in order to compare the proposed model with other models in the literature. However, changing the limits will result in changing the complexity and search time of the algorithms, which may or may not change the results as the used algorithms are known for their stability and accuracy; besides, one needs to follow the same used limits in order to compare and validate the results. These constraints are based on the maximum generation by one solar cell, cell number, and the material used.

Table 2. Parameter constraints.

	PWP-201					**R.T.C. France**				
	I_0*10^{-6}	R_s	R_{sh}	**N**	I_{ph}	I_0*10^{-6}	R_s	R_{sh}	**n**	I_{ph}
Lower limit	0	0	0	1	0	0	0	0	1	0
Upper limit	50	2	1000	50	2	1	0.5	100	2	1

The obtained values by using the entire dataset were used as the global optimum solution for the modules, which are also compared by the values obtained in literature. Therefore, the models which use these global optimum values were considered as reference models.

After finding the optimum values using only three data points, the predicted output current was compared to the actual measurements and the error was also compared with the results achieved by the reference models.

3. Results and Discussion

The experimental data of R.T.C. France cells and PWP-201 module are given in Tables 4 and 6. The first step is to use the experimental data to find the optimal solutions of the five parameters and to compare them with the other studies; then, these values were considered as the optimal values and used as a reference to evaluate the proposed methodology.

First of all, R.T.C France data were used for validating the proposed methods. The optimization results of PSO were (0.3218×10^{-6}, 0.0364, 53.4489, 1.4808, and 0.7608) for the parameters (I_0, R_s, R_{sh}, n, and I_{ph}), respectively, with an RMSE equal to 9.8636×10^{-4}. This was achieved by PSO using five swarms and the algorithm converged within 0.605784 s. However, GA estimated the values (0.3231, 0.0364, 53.7378, 1.4812, and 0.7608) for the same parameters, respectively, with an RMSE equal to 9.8602×10^{-4}. This was achieved by GA using a population size equal to 20 and the algorithm converged within 1.035257 s. A comparison of these results with previous studies, as shown in Table 3, showed similar values have been estimated in the literature. Indeed, GA provides more accurate results than PSO, but requires more time to converge.

As shown in Table 3, the estimated parameters of all techniques were almost equal with minor variations in some cases. Therefore, based on these values, a baseline model was considered as a reference and the proposed methodology was validated by comparing the performance of the new model to the baseline model.

After that, both PSO and GA were used to do the same, but considering only three data points given by the manufacturing datasheet, which are the short circuit current I_{sc}, where the output of the circuit is shorted and the voltage is equal to zero, the open-circuit voltage V_{oc}, where the output of the circuit is open and the current is equal to zero, and, finally the maximum power point. These three points are available for all PV panels, in contrast to the measured data. The results, as shown in Table 3, showed that PSO achieved better accuracy, 9.6481×10^{-8}, than GA. Note that the values of I_0 and R_{sh} were slightly

different from the reference model due to using only three points and due to setting a wide range of constraints for these two parameters while optimizing. Moreover, the RMSE was lower as compared with the reference model due to using fewer points for evaluation. Therefore, in order to validate the models accurately, further assessment for PSO using the experimental values was carried out.

Table 3. Comparison of the results of different algorithms on RTC France cell.

Algorithm	$I_0 \times 10^{-6}$	R_s	R_{sh}	n	I_{ph}	RMSE $\times 10^{-4}$
GA (This Study)	0.3231	0.0364	53.7378	1.4812	0.7608	9.8602
PSO (This Study)	0.3218	0.0364	53.6067	1.4808	0.7608	9.8636
PCE [35]	0.323021	0.036377	53.718525	1.481074	0.760776	9.86022
ABC [36]	0.3251	0.0364	53.6433	1.4817	0.7608	9.8620
CSO [37]	0.3230	0.03638	53.7185	1.48118	0.76078	9.8602
BMO [38]	0.32479	0.03636	53.8716	1.48173	0.76077	9.8608
ABC-DE [39]	0.32302	0.03637	53.7185	1.47986	0.76077	9.8602
With Three Points						
GA	0.4696	0.0285	38.2219	1.5207	0.7606	1.4153×10^{-3}
PSO	0.2994	0.0375	67.4972	1.4733	0.7604	9.6481×10^{-4}

The results of the proposed PSO using three data points were compared with the outputs of PSO using all data and the result of the WHHO algorithm [14], ABC [36], and BMO [38] in Table 4, where I_{pred} is the estimated current. The results showed close results of the proposed model to other models with slightly more error in the range of 10–4, which makes it reasonable.

Table 4. Experimental I-V dataset for R.T.C. France solar cell [14].

S.N	Experimental Data		WH [14]		ABC [36]		BMO [38]		PSO Reference Model		PSO with 3 Data Points	
	VL	IL	I_{pred}	Error	I_{pred}	Error	I_{pred}	Error	I_{pred}	Error	I_{pred}	Error
1	−0.2057	0.764	0.764067	−0.000088	0.7641	−0.0001	0.763965	0.00004	0.76412	0.000119	0.76302	−0.000977
2	−0.1291	0.762	0.762647	−0.000849	0.7626	−0.0006	0.762593	−0.00059	0.76269	0.000691	0.76189	−0.00011
3	−0.0588	0.7605	0.761344	−0.001109	0.7613	−0.0008	0.761334	−0.00083	0.76138	0.000881	0.76085	0.000349
4	0.0057	0.7605	0.760148	0.000462	0.7601	0.0004	0.760177	0.00032	0.76018	−0.000323	0.75989	−0.000607
5	0.0646	0.76	0.759054	0.001246	0.759	0.0010	0.759117	0.00088	0.75908	−0.000924	0.75902	−0.000982
6	0.1185	0.759	0.758044	0.001259	0.758	0.0010	0.758135	0.00087	0.75806	−0.000939	0.75821	−0.00079
7	0.1678	0.757	0.757096	−0.000127	0.7571	−0.0001	0.757205	−0.00021	0.75711	0.000108	0.75745	0.000447
8	0.2132	0.757	0.75615	0.001123	0.7561	0.0009	0.756262	0.00074	0.75616	−0.000844	0.75667	−0.000329
9	0.2545	0.7555	0.755097	0.000532	0.755	0.0005	0.755193	0.00031	0.7551	−0.000399	0.75578	0.000277
10	0.2924	0.754	0.753676	0.000428	0.7536	0.0004	0.753732	0.00027	0.75368	−0.000323	0.7545	0.000503
11	0.3269	0.7505	0.751401	−0.001199	0.7513	−0.0008	0.751397	−0.00090	0.7514	0.000904	0.75237	0.001865
12	0.3585	0.7465	0.74736	−0.001151	0.7473	−0.0008	0.747287	−0.00079	0.74737	0.000868	0.74844	0.001941
13	0.3873	0.7385	0.740107	−0.002171	0.7401	−0.0016	0.739973	−0.00147	0.74013	0.001633	0.74128	0.002776
14	0.4137	0.728	0.727403	0.00082	0.7273	0.0007	0.727243	0.00076	0.7274	−0.0006	0.72853	0.000532
15	0.4373	0.7065	0.706954	−0.000642	0.7069	−0.0004	0.706819	−0.00032	0.707	0.00049	0.708	0.001488
16	0.459	0.6755	0.67529	0.00031	0.6752	0.0003	0.675224	0.00028	0.6753	−0.0002	0.676	0.000478
17	0.4784	0.632	0.630875	0.001782	0.6307	0.0013	0.630895	0.00111	0.63077	−0.00123	0.63095	−0.001055
18	0.496	0.573	0.572071	0.001623	0.5718	0.0012	0.572157	0.00084	0.57194	−0.00106	0.57145	−0.001546
19	0.5119	0.499	0.49948	−0.000962	0.4995	−0.0005	0.499589	−0.00059	0.49961	0.000606	0.49844	−0.000558
20	0.5265	0.413	0.413485	−0.001173	0.4136	−0.0006	0.413569	−0.00057	0.41364	0.000637	0.41189	−0.001114

Table 4. *Cont.*

S.N	Experimental Data		WH [14]		ABC [36]		BMO [38]		PSO Reference Model		PSO with 3 Data Points	
	VL	IL	I_{pred}	Error	I_{pred}	Error	I_{pred}	Error	I_{pred}	Error	I_{pred}	Error
21	0.5398	0.3165	0.317214	−0.002251	0.3175	−0.0010	0.317245	−0.00074	0.3175	0.0001	0.31544	−0.00106
22	0.5521	0.212	0.212101	−0.000477	0.2121	−0.0001	0.212075	−0.00008	0.21213	0.000131	0.21021	−0.001794
23	0.5633	0.1035	0.102722	0.00757	0.1022	0.0013	0.102659	0.00084	0.10223	−0.001268	0.10097	−0.002527
24	0.5736	−0.0100	−0.009246	0.081536	−0.0086	−0.0014	−0.00931	−0.00069	−0.0087	0.001279	−0.0086	0.00136
25	0.5833	−0.1230	−0.124378	−0.011080	−0.1254	0.0024	−0.12439	0.00139	−0.1255	−0.002487	−0.12348	−0.000482
26	0.59	−0.2100	−0.209190	0.00387	−0.2084	−0.0016	−0.20914	−0.00086	−0.2084	0.001577	−0.20447	0.00553
	RMSE		**9.8602×10^{-4}**		**9.8629×10^{-4}**		**9.8608×10^{-4}**		**9.8624×10^{-4}**		**16×10^{-4}**	

Moreover, the proposed model output current was compared to the outputs of the reference model and other models from the literature, and the proposed model showed similar behavior as compared to the other models. The boxplot in Figure 8 shows the variation of the current for the models, which were similar in all models. Figure 9 represents the boxplot of the variation in the error for each model. The figure shows that the BMO model was more stable than other models; however, the proposed model was still able to achieve accurate results with a slight difference.

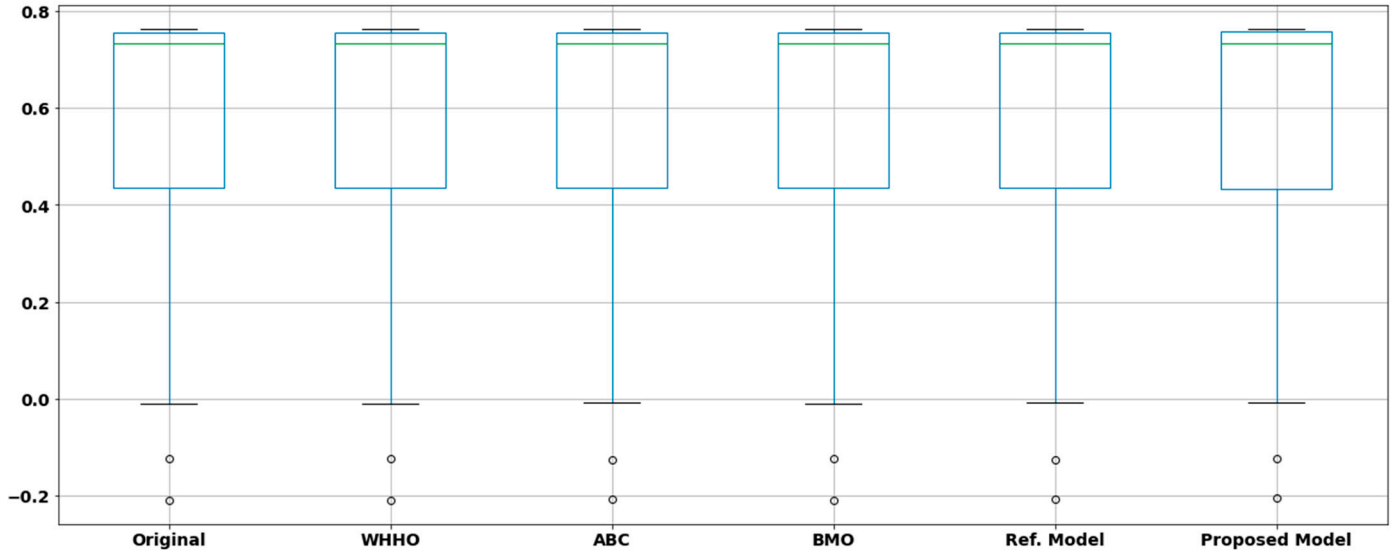

Figure 8. Boxplot of the current variation of the original data, proposed model, and other models from the literature (WHHO [14], ABC [36], and BMO [38]) regarding the R.T.C. France model.

For further validation, the proposed model was compared with the reference model, by comparing both I-V and P-V characteristic curves using Simulink. As indicated in Figure 10, the I-V and P-V curves of the reference model and the proposed model were identical, with a difference of only 7.6212×10^{-4} RMSE between the I-V lines under the standard conditions. This implies that the proposed model is just as accurate as the reference model.

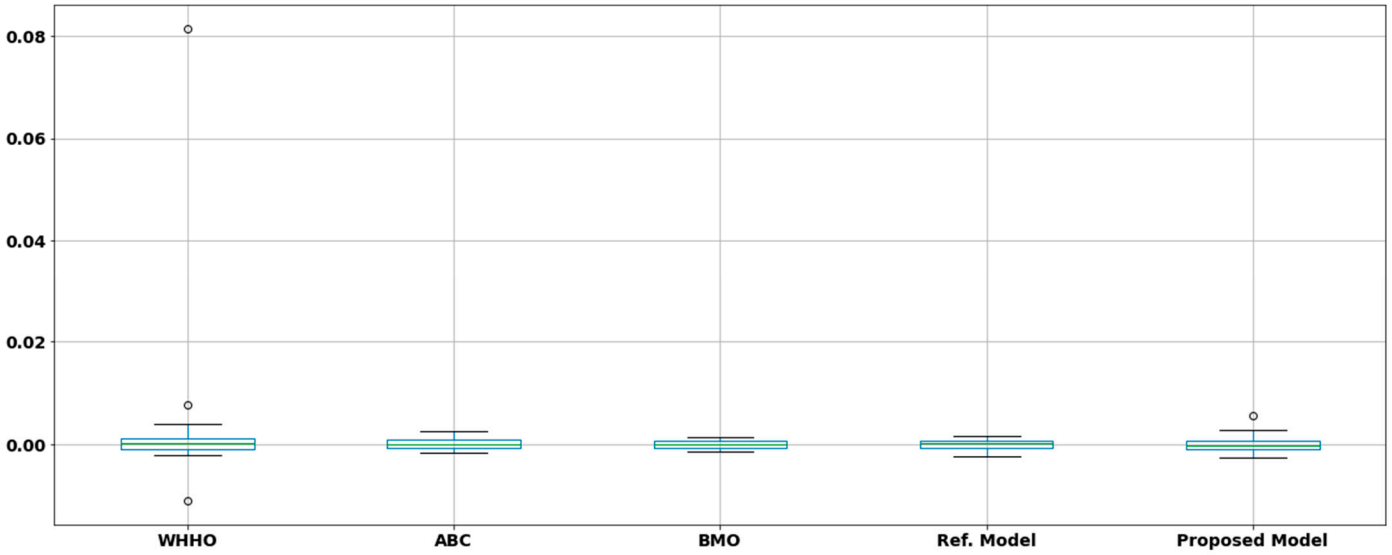

Figure 9. Boxplot of the error in current for the proposed model and other models from the literature (WHHO [14], ABC [36], and BMO [38]) compared to the original data regarding the R.T.C. France model.

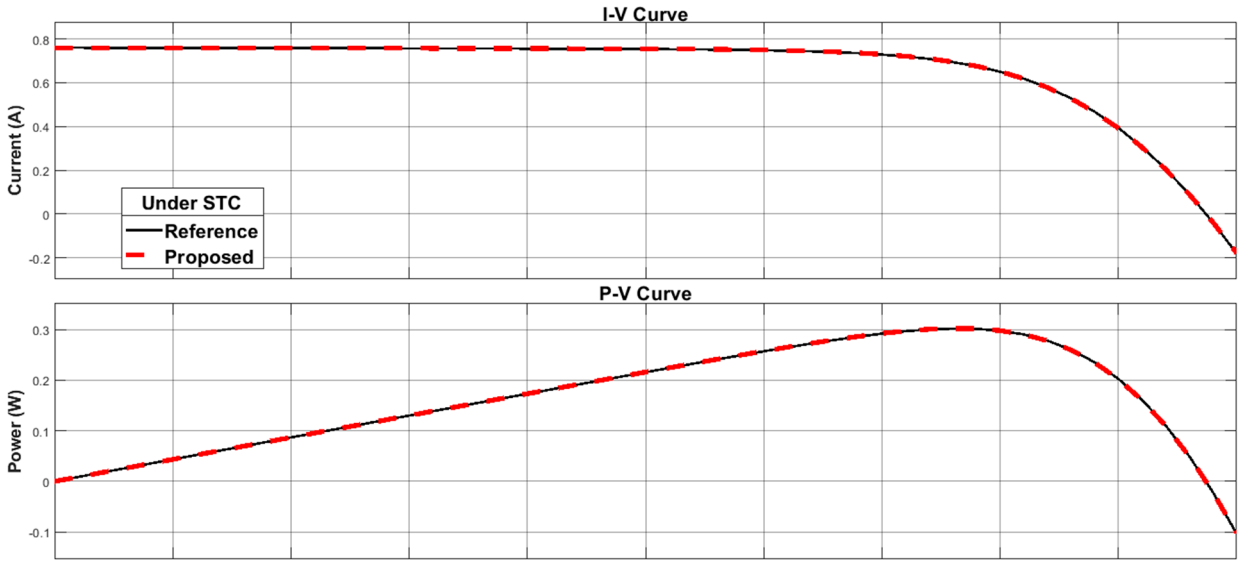

Figure 10. I−V and P−V curves for the reference and the proposed model under STC.

Moreover, the models were compared under different solar radiation values, as shown in Figures 11–14; it is clear from these curves that under all conditions the proposed model followed the pattern of the reference model with very little error. The I-V lines of the proposed and the reference models were compared under different conditions using RMSE, which was found to be equal to 0.0012, 0.0017, 0.0025, and 0.0032 under 800, 600, 400, and 200 W/m^2 solar radiations, respectively. Therefore, it can be noticed that the error increased when the radiation decreased; however, it is still a reasonable range of error.

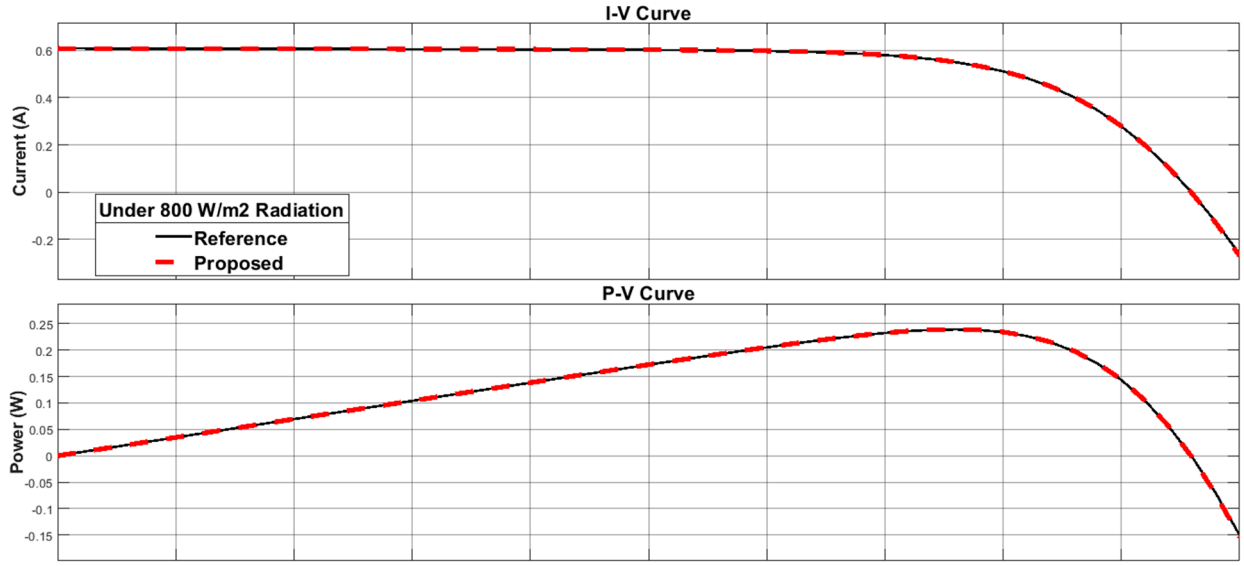

Figure 11. I−V and P−V curves for the reference and the proposed model under 800 W/m^2 radiation.

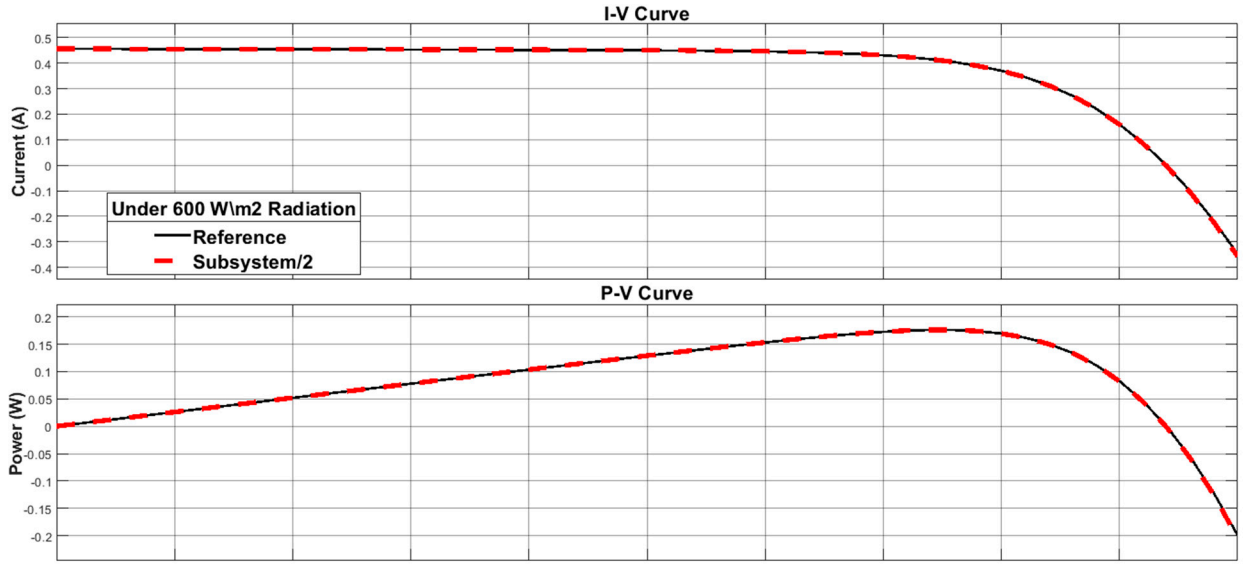

Figure 12. I−V and P−V curves for the reference and the proposed model under 600 W/m^2 radiation.

The comparison between the reference model and the proposed model was also carried out using Taylor graph, Figure 15, which represents how both models are close to the reference value, being the actual measurements. Moreover, the mean bias error (MBE) and mean absolute error (MAE) of the proposed model were calculated and found to be 0.001213 and 0.00014, respectively. In addition, the correlation between the predictions and the actual measurements is plotted in Figure 16, where the R value was very close to 1.

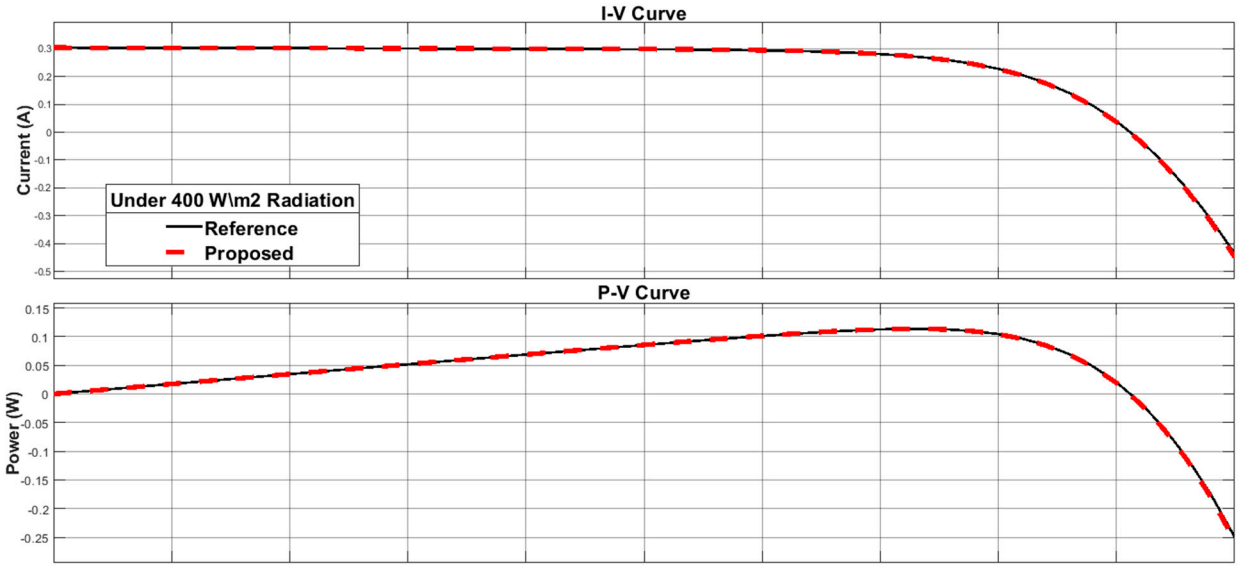

Figure 13. I−V and P−V curves for the reference and the proposed model under 400 W/m^2 radiation.

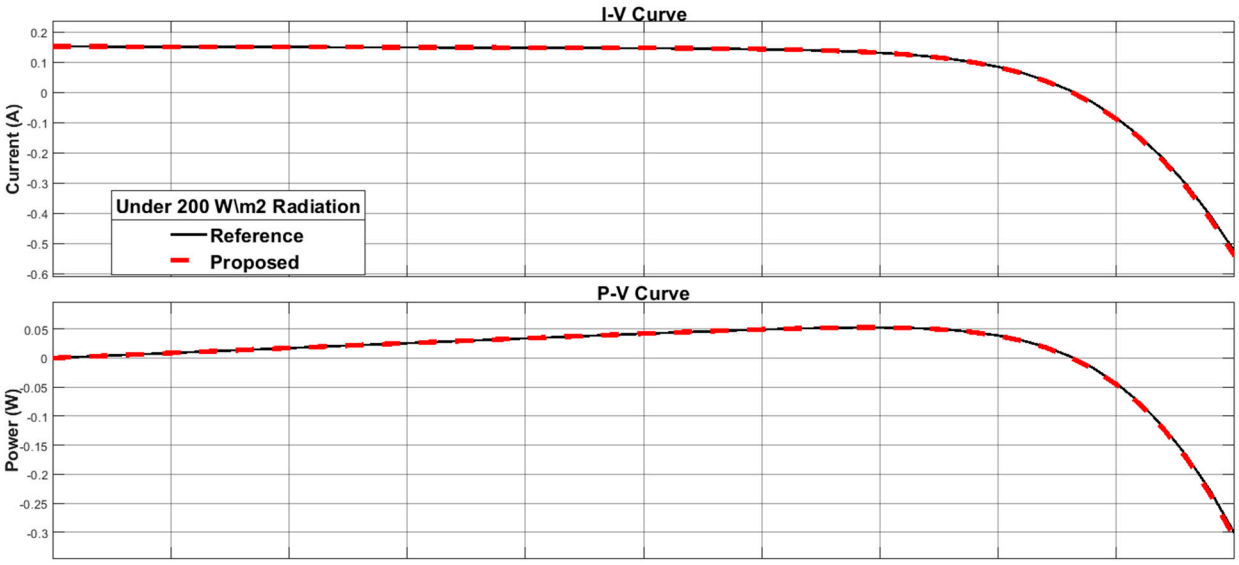

Figure 14. I−V and P−V curves for the reference and the proposed model under 200 W/m^2 radiation.

To make sure that this methodology does not work only with single-cell modules, another module, the PWM201 PV module, with 36 solar cells was used and the manufacturing data of the module are shown in Table 1. The same objective function was used, and the constraints are given in Table 2. Both PSO and GA were applied for this module as well. The results, given in Table 5, showed that both techniques had similar accuracy when using the full dataset for training. However, PSO (1.9172×10^{-8}) showed less error compared with GA (1.2167×10^{-7}) when using only three points.

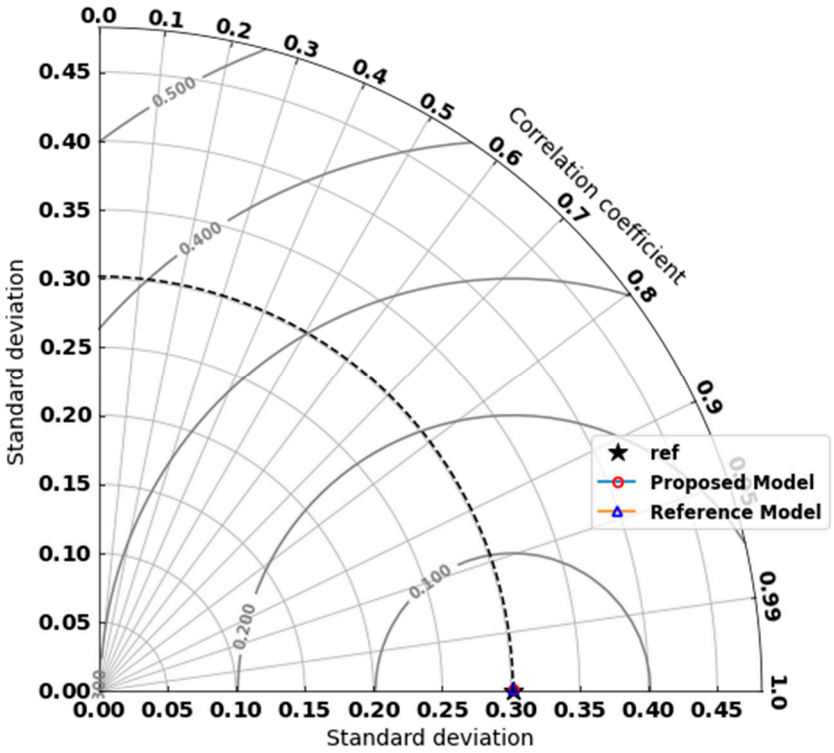

Figure 15. Taylor Diagram showing the standard deviation, correlation, and RMSE of the proposed model and the reference model.

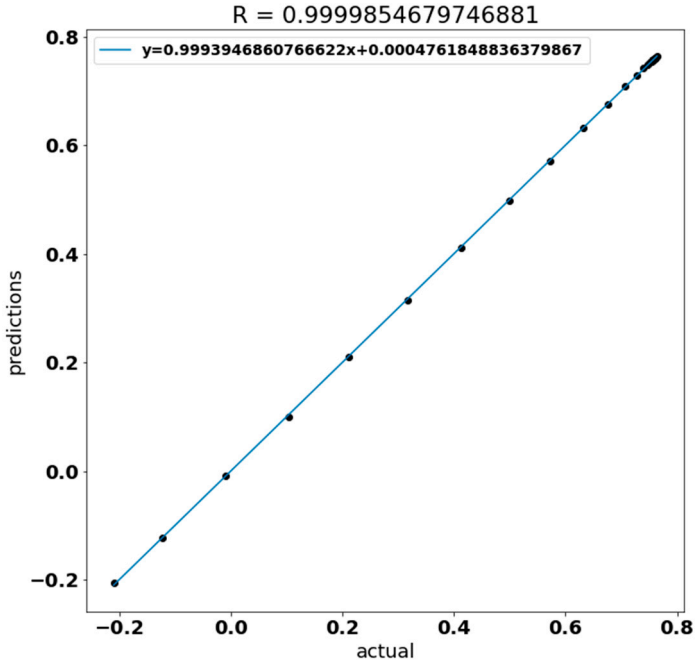

Figure 16. Correlation between the predicted current and the actual measurements.

Table 5. Comparison of the proposed methodology and other methods in finding the PWM201 module's parameters.

Algorithm	$I_0 \times 10^{-6}$	R_s	R_{sh}	n	I_{ph}	RMSE $\times 10^{-3}$
GA (This Study)	3.4650	1.2018	975.7689	1.3507	1.0305	2.4
PSO (This Study)	3.4203	1.2029	951.6120	1.3493	1.0307	2.4
WHHO [14]	3.482109	1.201274	981.905230	1.349987	1.030514	2.42507
EHHO [42]	3.459968	1.201853	971.276026	1.349314	1.030583	2.42516
JAYA [43]	3.4931	1.2014	1000	1.3514	1.0307	2.42778
STLBO [44]	3.4824	1.2013	982.0387	1.3511	1.0305	2.42507
TLABC [45]	3.4826	1.2013	982.1815	1.3512	1.0305	2.42507
Using only three points						
GA	1.0023	1.4927	858.7274	1.2296	1.0318	1.2167×10^{-4}
PSO	4.8783	1.0698	741.0845	1.3889	1.0315	1.9172×10^{-5}

To ensure that the proposed models using PSO and GA with three data points have reasonable behavior compared to the reference one, both models were tested using the experimental dataset and the output is shown in Table 6 and compared to the reference model, in addition to WHHO [14], JAYA [43], and EHHO [42] from the literature. RMSE for all methods were compared and it was found that PSO achieved better accuracy (0.0093) than GA (0.0196); however, it had a lower accuracy compared with the reference model, which was trained using the full dataset points (0.0024) where the difference was in the range of 10–3, which makes it reasonable for applications where such an error does not matter.

Table 6. Comparison of the estimated output current for the the proposed methodology and the reference model for the PWM201 modules.

S.N	Experimental data		WHHO [14]		JAYA [43]		EHHO [42]		PSO Output Using Three Data Points		GA Output Using Three Data Points	
	V	I	I_{pred}	Error	I_{pred}	Error	I_{pred}	Error	I_{pred}	Error	I_{pred}	Error
1	0.1248	1.0315	1.029122	0.00231	1.02911964	0.00238036	1.0286	0.0029	1.0298	−0.001665	1.0299	−0.001641
2	1.8093	1.03	1.027385	0.002546	1.02738133	0.00261867	1.0269	0.003	1.0275	−0.002464	1.0279	−0.002112
3	3.3511	1.026	1.025742	0.000251	1.02574186	0.00025814	1.0255	0.0005	1.0254	−0.000623	1.0261	5.9×10^{-5}
4	4.7622	1.022	1.024104	−0.00205	1.02410704	0.00210704	1.0239	0.0019	1.0233	0.001254	1.0243	0.002301
5	6.0538	1.018	1.022283	−0.00419	1.02229155	0.00429155	1.0222	0.0042	1.021	0.002973	1.0225	0.004467
6	7.2364	1.0155	1.019917	−0.00433	1.01993032	0.00443032	1.0199	0.0044	1.0182	0.002661	1.0203	0.00475
7	8.3189	1.014	1.016351	−0.00231	1.01636269	0.00236269	1.0164	0.0024	1.0142	0.000165	1.017	0.003042
8	9.3097	1.01	1.010491	−0.00049	1.01049575	0.00049575	1.0106	0.0006	1.0079	−0.002066	1.0118	0.001755
9	10.2163	1.0035	1.000679	0.00282	1.00062866	0.00287134	1.0007	0.0028	0.9979	−0.00564	1.0026	−0.000938
10	11.0449	0.988	0.984653	0.003399	0.98454823	0.00345177	0.9847	0.0033	0.9819	−0.006115	0.9869	−0.001068
11	11.8018	0.963	0.959697	0.003441	0.95952173	0.00347827	0.9596	0.0034	0.9575	−0.005518	0.9616	−0.001418
12	12.4929	0.9255	0.923049	0.002656	0.92283908	0.00266092	0.9229	0.0025	0.9221	−0.003365	0.9232	−0.002343
13	13.1231	0.8725	0.872588	−0.0001	0.87260009	0.00010009	0.8727	0.0002	0.874	0.001497	0.8694	−0.003142
14	13.6983	0.8075	0.80731	0.000235	0.80727477	0.00022523	0.8074	0.0001	0.8115	0.00401	0.7985	−0.009035
15	14.2221	0.7265	0.727958	−0.002	0.72833695	0.00183695	0.7284	0.0019	0.7357	0.009169	0.713	−0.013542
16	14.6995	0.6345	0.636466	−0.00309	0.63713835	0.00263835	0.6372	0.0027	0.6474	0.012892	0.6152	−0.019293
17	15.1346	0.5345	0.535696	−0.00223	0.53621321	0.00171321	0.5362	0.0017	0.5487	0.014183	0.5091	−0.025423
18	15.5311	0.4275	0.428816	−0.00307	0.42951127	0.00201127	0.4295	0.002	0.4429	0.015351	0.4002	−0.027318
19	15.8929	0.3185	0.318669	−0.00053	0.31877424	0.00027424	0.3188	0.0003	0.3315	0.012952	0.2907	−0.027798
20	16.2229	0.2085	0.207857	0.003093	0.20738914	0.00111086	0.2074	0.0011	0.2176	0.009058	0.1848	−0.023694
21	16.5241	0.101	0.098354	0.026901	0.09616674	0.00483326	0.0962	0.0048	0.1021	0.001117	0.0829	−0.018135
22	16.7987	−0.008	−0.00817	−0.02073	−0.0083257	0.00032571	−0.0082	0.0002	−0.0089	−0.000887	−0.007	0.000956
23	17.0499	−0.111	−0.11097	0.000284	−0.1109366	0.00006337	−0.1108	0.0002	−0.1193	−0.008342	−0.0924	0.018616
24	17.2793	−0.209	−0.20912	−0.00056	−0.2092472	0.00024715	−0.2091	8.80×10^{-5}	−0.2268	−0.017807	−0.1708	0.038223
25	17.4885	−0.303	−0.30202	0.003237	−0.3008631	0.00213691	−0.3007	0.0023	−0.3288	−0.025837	−0.2399	0.063061
RMSE			2.42507×10^{-3}		2.42507×10^{-3}		2.42516×10^{-3}		9.3×10^{-3}		19.6×10^{-3}	

For further comparison, the proposed model output current was compared to the outputs of the reference model and other models from the literature, as shown in Figures 17 and 18, and the proposed model showed similar behavior as compared to the other models. The boxplot in Figure 17 shows the variation of the output current of the models and it was similar for all with a slight difference in the negative current. Figure 18 represents the

boxplot of the variation in the error for each model. The figure shows that WHHO model was more accurate than other models; however, the proposed model was still able to achieve accurate results with a slight difference.

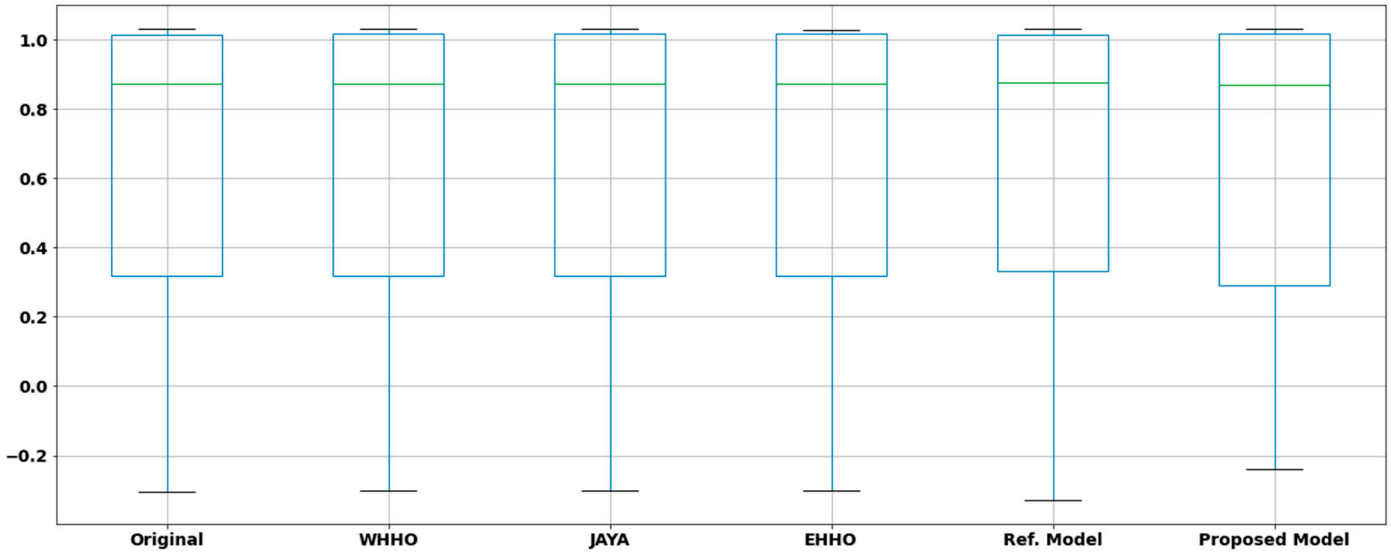

Figure 17. Boxplot of the current variation of the original data, proposed model, and other models from the literature (WHHO [14], JAYA [41], and EHHO [40]) regarding the PWM201 model.

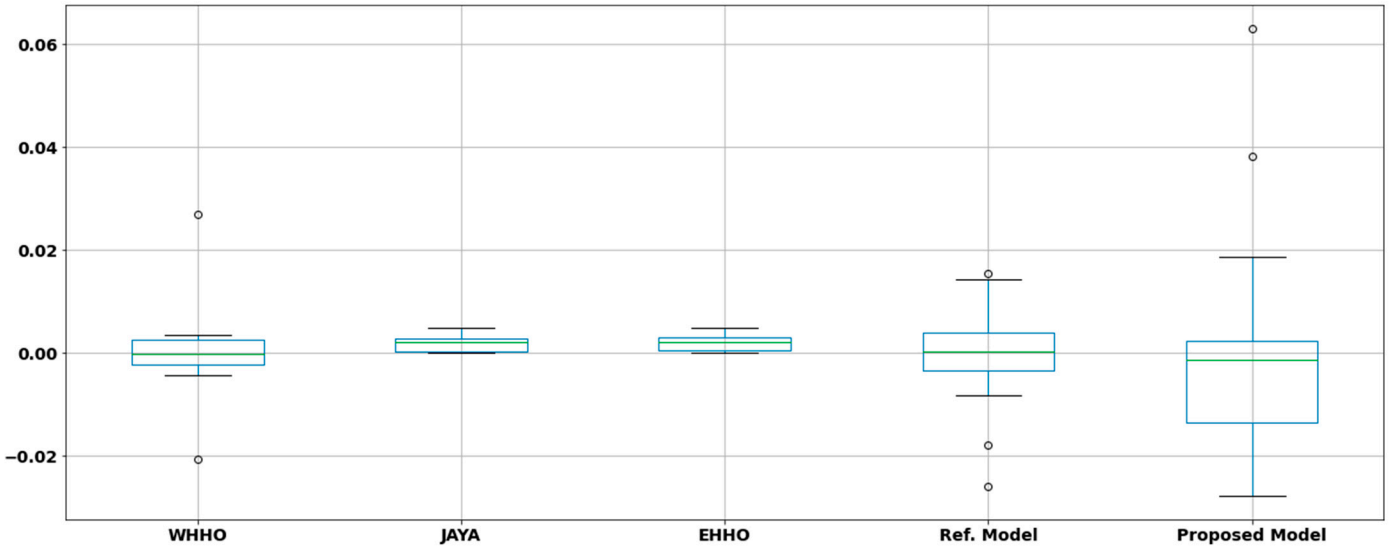

Figure 18. Boxplot of the error in current for the proposed model and other models from the literature (WHHO [14], JAYA [41], and EHHO [40]) compared to the original data regarding the PWM201 model.

The comparison between the reference model and the proposed model was also carried out using a Taylor graph, Figure 19, which represents that the proposed model slightly differed from the actual measurements. Moreover, the MBE and MAE of the proposed model were found to be 0.01256 and −0.00156, respectively. In addition, the correlation between the predictions and the actual measurements is plotted in Figure 20, where the R value was very close to 1.

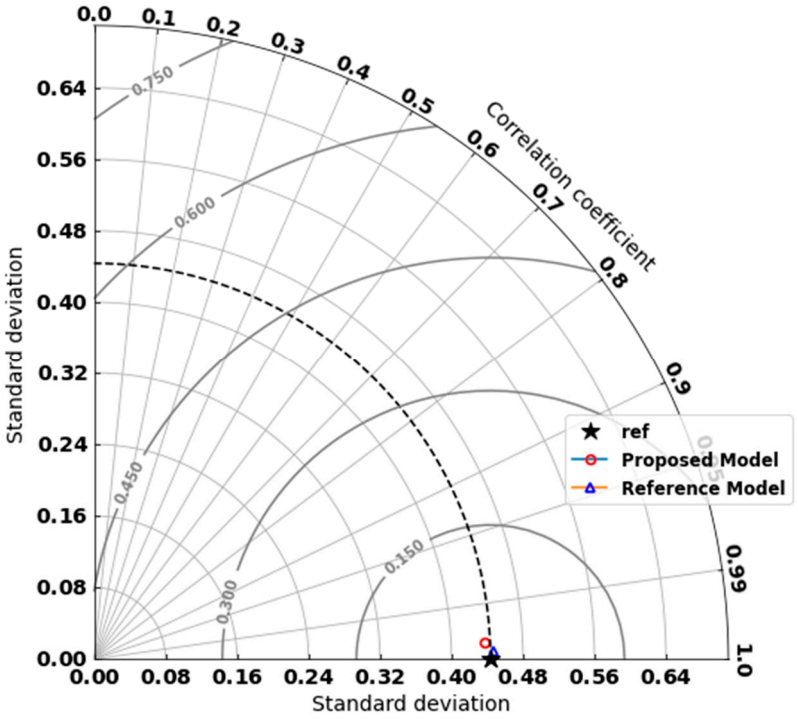

Figure 19. Taylor Diagram showing the standard deviation, correlation, and RMSE of the proposed model and the reference model.

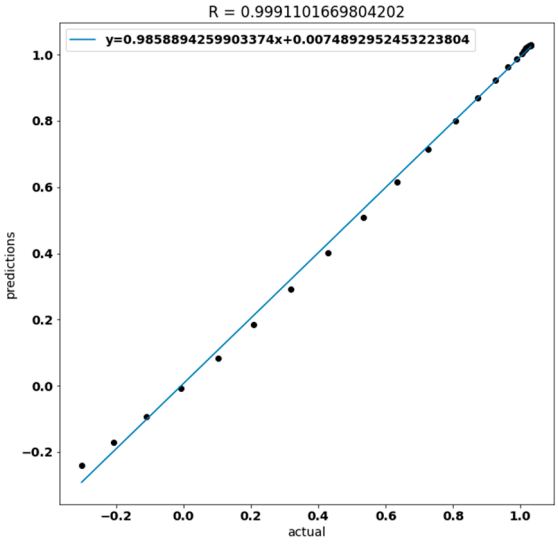

Figure 20. Correlation between the predicted current and the actual measurements.

As the proposed model works efficiently for both R.T.C France solar cell and PWP201 modules, it will work for other types of modules and can be further experimented with in future studies. However, these two types of solar cells/modules were selected due to the availability of the experimental data for validation only, whereas the proposed method does not require any experimental data, which is promising for commercial modules for which no experimental datasets are available.

4. Conclusions and Follow-Up Research

A new model for parameter estimation of solar modeling for reliable energy management using metaheuristic algorithms was presented for the newly established commercial PV microgrids. In this study, a new model was presented to predict solar cells' power

generation. The developed model was validated using experimental data. Both genetic algorithm (GA) and particle swarm algorithm (PSO) were investigated to estimate the values of the solar cell parameters. The developed new model was tested under different solar irradiance conditions and compared with a reference model and was found to be accurate under all conditions. Based on the study, the following conclusions are drawn:

1. The results showed that using the full data points, both GA and PSO algorithms obtained reasonable optimization results, which led to similar or sometimes better results than those obtained in previous studies.
2. The proposed model considers only three measurements, taken from the manufacturer datasheets, and this makes it a very effective methodology to estimate solar cell parameters for all commercial modules as there is no need to set up any experimental measurements for newly established PV-based microgrids.
3. Testing the proposed model on the R.T.C France solar cell proved that this new model is able to perform as accurately as the reference model under all conditions; however, the error increased when the solar radiation decreased where the maximum RMSE detected under 200 W/m^2 solar radiation was 0.0032 as compared with 7.6212×10^{-4} under standard conditions.
4. Using PWP201 for validation also showed that this model can be used for all commercial solar modules.

This model can be used for all types of photovoltaic systems, especially commercial microgrids for which no long-term experimental data are available and provides accurate results, which are comparable to modeling with multiple measurement data points. This model can also be utilized for maximum power point tracking research and development in addition to the analysis of PV-based microgrids to facilitate the management of the microgrids, which will be discussed in a follow-up study.

Author Contributions: Conceptualization, S.T., S.S.C., H.M., M.A.A. and T.S.U.; Data curation, S.T., S.S.C., H.M. and T.S.U.; Formal analysis, S.T., S.S.C., H.M., M.A.A. and T.S.U.; Funding acquisition, H.M. and M.A.A.; Investigation, S.T., S.S.C., H.M., M.A.A. and T.S.U.; Methodology, S.T., S.S.C., H.M., M.A.A. and T.S.U.; Project administration, H.M., M.A.A. and T.S.U.; Resources, S.T., S.S.C., H.M. and T.S.U.; Software, S.T., S.S.C., M.A.A. and T.S.U.; Supervision, S.S.C., H.M. and T.S.U.; Validation, S.T., S.S.C., H.M. and M.A.A.; Visualization, S.T., S.S.C. and H.M.; Writing—original draft, S.T., H.M. and M.A.A.; Writing—review & editing, S.S.C. and T.S.U. All authors have read and agreed to the published version of the manuscript.

Funding: The authors extend their appreciation to the Researchers Supporting Project at King Saud University, Riyadh, Saudi Arabia, for funding this research work through the project number RSP-2021/278.

Institutional Review Board Statement: Not applicable.

Informed Consent Statement: Not applicable.

Data Availability Statement: The data will be made available on request to authors.

Acknowledgments: The authors would like to acknowledge the support from Solar Photovoltaic Research Group, Centre of Excellence in Energy Science and Technology, Shoolini University, Solan, Himachal Pradesh, India; support from Department of Electrical Power Engineering, Faculty of Electrical Engineering, University Technology Malaysia (UTM), Johor Bahru, Malaysia; support from Department of Electrical Engineering, College of Engineering, King Saud University, Riyadh, Saudi Arabia; support from Fukushima Renewable Energy Institute, AIST (FREA), National Institute of Advanced Industrial Science and Technology (AIST), Japan and support from Intelligent Prognostic Private Limited Delhi, India researcher's supporting Project.

Conflicts of Interest: The authors declare no conflict of interest.

References

1. Malik, P.; Chandel, S.S. A new integrated single-diode solar cell model for photovoltaic power prediction with experimental validation under real outdoor conditions. *Int. J. Energy Res.* **2020**, *45*, 759–771. [CrossRef]
2. Tamrakar, V.; Gupta, S.C.; Sawle, Y. Single-Diode and Two-Diode Pv Cell Modeling Using Matlab For Studying Characteristics of Solar Cell Under Varying Conditions. *Electr. Comput. Eng. Int. J.* **2015**, *4*, 67–77. [CrossRef]
3. Malik, P.; Chandel, R.; Chandel, S.S. A power prediction model and its validation for a roof top photovoltaic power plant considering module degradation. *Sol. Energy* **2021**, *224*, 184–194. [CrossRef]
4. Rawat, R.; Chandel, S.S. Review of Maximum-Power-Point Tracking Techniques for Solar-Photovoltaic Systems. *Energy Technol.* **2013**, *1*, 438–448. [CrossRef]
5. Sharma, V.; Chandel, S.S. Performance and degradation analysis for long term reliability of solar photovoltaic systems: A review. *Renew. Sustain. Energy Rev.* **2013**, *27*, 753–767. [CrossRef]
6. Rasheed, M.; Alabdali, O.; Shihab, S. A New Technique for Solar Cell Parameters Estimation of the Single-Diode Model. *J. Phys. Conf. Ser.* **2021**, *1879*, 032120. [CrossRef]
7. Rasheed, M.; Al-Darraji, M.N.; Shihab, S.; Rashid, A.; Rashid, T. The numerical Calculations of Single-Diode Solar Cell Modeling Parameters. *J. Phys. Conf. Ser.* **2021**, *1963*, 1. [CrossRef]
8. Zagrouba, M.; Sellami, A.; Bouaïcha, M.; Ksouri, M. Identification of PV solar cells and modules parameters using the genetic algorithms: Application to maximum power extraction. *Sol. Energy* **2010**, *84*, 860–866. [CrossRef]
9. El-Naggar, K.M.; AlRashidi, M.R.; AlHajri, M.F.; Al-Othman, A.K. Simulated Annealing algorithm for photovoltaic parameters identification. *Sol. Energy* **2012**, *86*, 266–274. [CrossRef]
10. Messaoud, R.B. Extraction of uncertain parameters of single-diode model of a photovoltaic panel using simulated annealing optimization. *Energy Rep.* **2020**, *6*, 350–357. [CrossRef]
11. Soon, J.J.; Low, K.S. Photovoltaic model identification using particle swarm optimization with inverse barrier constraint. *IEEE Trans. Power Electron.* **2012**, *27*, 3975–3983. [CrossRef]
12. Cortez, R.; Garrido, R.; Mezura-Montes, E. Spectral Richness PSO algorithm for parameter identification of dynamical systems under non-ideal excitation conditions. *Appl. Soft Comput.* **2022**, *128*, 109490. [CrossRef]
13. Abdel-Basset, M.; Mohamed, R.; Chakrabortty, R.K.; Sallam, K.; Ryan, M.J. An efficient teaching-learning-based optimization algorithm for parameters identification of photovoltaic models: Analysis and validations. *Energy Convers. Manag.* **2020**, *227*, 113614. [CrossRef]
14. Naeijian, M.; Rahimnejad, A.; Ebrahimi, S.M.; Pourmousa, N.; Gadsden, S.A. Parameter estimation of PV solar cells and modules using Whippy Harris Hawks Optimization Algorithm. *Energy Rep.* **2021**, *7*, 4047–4063. [CrossRef]
15. Ebrahimi, S.M.; Salahshour, E.; Malekzadeh, M.; Gordillo, F. Parameters identification of PV solar cells and modules using flexible particle swarm optimization algorithm. *Energy* **2019**, *179*, 358–372. [CrossRef]
16. Awadallah, M.A. Variations of the bacterial foraging algorithm for the extraction of PV module parameters from nameplate data. *Energy Convers. Manag.* **2016**, *113*, 312–320. [CrossRef]
17. AlHajri, M.F.; El-Naggar, K.M.; AlRashidi, M.R.; Al-Othman, A.K. Optimal extraction of solar cell parameters using pattern search. *Renew. Energy* **2012**, *44*, 238–245. [CrossRef]
18. Diab, A.A.Z.; Sultan, H.M.; Aljendy, R.; Al-Sumaiti, A.S.; Shoyama, M.; Ali, Z.M. Tree Growth Based Optimization Algorithm for Parameter Extraction of Different Models of Photovoltaic Cells and Modules. *IEEE Access* **2020**, *8*, 119668–119687. [CrossRef]
19. Iab, A.A.Z.D.; Sultan, H.M.; Do, T.D.; Kamel, O.M.; Mossa, M.A. Coyote Optimization Algorithm for Parameters Estimation of Various Models of Solar Cells and PV Modules. *IEEE Access* **2020**, *8*, 111102–111140. [CrossRef]
20. Abdel-Basset, M.; Mohamed, R.; Mirjalili, S.; Chakrabortty, R.K.; Ryan, M.J. Solar photovoltaic parameter estimation using an improved equilibrium optimizer. *Sol. Energy* **2020**, *209*, 694–708. [CrossRef]
21. Wang, M.; Zhao, X.; Heidari, A.A.; Chen, H. Evaluation of constraint in photovoltaic models by exploiting an enhanced ant lion optimizer. *Sol. Energy* **2020**, *211*, 503–521. [CrossRef]
22. Louzazni, M.; Khouya, A.; Amechnoue, K.; Gandelli, A.; Mussetta, M.; Craciunescu, A. Metaheuristic algorithm for photovoltaic parameters: Comparative study and prediction with a Firefly algorithm. *Appl. Sci.* **2018**, *8*, 339. [CrossRef]
23. El-Dabah, M.A.; El-Sehiemy, R.A.; Becherif, M.; Ebrahim, M.A. Parameter estimation of triple diode photovoltaic model using an artificial ecosystem-based optimizer. *Int. Trans. Electr. Energy Syst.* **2021**, *31*, e13043. [CrossRef]
24. Ridha, H.M.; Hizam, H.; Mirjalili, S.; Othman, M.L.; Ya'Acob, M.E.; Ahmadipour, M.; Ismaeel, N.Q. On the problem formulation for parameter extraction of the photovoltaic model: Novel integration of hybrid evolutionary algorithm and Levenberg Marquardt based on adaptive damping parameter formula. *Energy Convers. Manag.* **2022**, *256*, 115403. [CrossRef]
25. Tajjour, S.; Garg, S.; Chandel, S.S.; Sharma, D. A novel hybrid artificial neural network technique for the early skin cancer diagnosis using color space conversions of original images. *Int. J. Imaging Syst. Technol.* 2022; Early View. [CrossRef]
26. Tajjour, S.; Chandel, S. Power Generation Forecasting of a Solar Photovoltaic Power Plant by a Novel Transfer Learning Technique with Small Solar Radiation and Power Generation Training Data Sets. *SSRN Electron. J.* 2022; Early View. [CrossRef]
27. Tajjour, S.; Chandel, S.S. A Novel Strategy for Solar Irradiance Forecasting Using Deep Learning Techniques and Validation for a Himalayan Location in India as a Case Study. *SSRN Electron. J.* 2022; Early View. [CrossRef]
28. Maleki, A.; Haghighi, A.; Assad, M.e.; Mahariq, I.; Nazari, M.A. A review on the approaches employed for cooling PV cells. *Sol. Energy* **2020**, *209*, 170–185. [CrossRef]

29. Ustun, T.S.; Nakamura, Y.; Hashimoto, J.; Otani, K. Performance analysis of PV panels based on different technologies after two years of outdoor exposure in Fukushima, Japan. *Renew. Energy* **2018**, *136*, 159–178. [CrossRef]
30. Yaqoob, S.J.; Saleh, A.L.; Motahhir, S.; Agyekum, E.B.; Nayyar, A.; Qureshi, B. Comparative study with practical validation of photovoltaic monocrystalline module for single and double diode models. *Sci. Rep.* **2021**, *11*, 1–14. [CrossRef]
31. Haldurai, L.; Madhubala, T.; Rajalakshmi, R. A Study on Genetic Algorithm and its Applications. *Int. J. Comput. Sci. Eng.* **2016**, *4*, 10. Available online: https://www.ijcseonline.org (accessed on 15 June 2022).
32. Holland, J.H. Genetic Algorithms. *Sci. Am.* **1992**, *4*, 66–72. [CrossRef]
33. Elsheikh, A.H.; Elaziz, M.A. Review on applications of particle swarm optimization in solar energy systems. *Int. J. Environ. Sci. Technol.* **2019**, *16*, 1159–1170. [CrossRef]
34. Ye, M.; Wang, X.; Xu, Y. Parameter extraction of solar cells using particle swarm optimization. *J. Appl. Phys.* **2009**, *105*, 094502. [CrossRef]
35. Zhang, Y.; Lin, P.; Chen, Z.; Cheng, S. A Population Classification Evolution Algorithm for the Parameter Extraction of Solar Cell Models. *Int. J. Photoenergy* **2016**, *2016*, 16–18. [CrossRef]
36. Oliva, D.; Cuevas, E.; Pajares, G. Parameter identification of solar cells using artificial bee colony optimization. *Energy* **2014**, *72*, 93–102. [CrossRef]
37. Guo, L.; Meng, Z.; Sun, Y.; Wang, L. Parameter identification and sensitivity analysis of solar cell models with cat swarm optimization algorithm. *Energy Convers. Manag.* **2016**, *108*, 520–528. [CrossRef]
38. Askarzadeh, A.; Rezazadeh, A. Extraction of maximum power point in solar cells using bird mating optimizer-based parameters identification approach. *Sol. Energy* **2013**, *90*, 123–133. [CrossRef]
39. Hachana, O.; Hemsas, K.E.; Tina, G.M.; Ventura, C. Comparison of different metaheuristic algorithms for parameter identification of photovoltaic cell/module. *J. Renew. Sustain. Energy* **2013**, *5*, 5. [CrossRef]
40. Fatema, N.; Malik, H. Data-Driven Occupancy Detection Hybrid Model Using Particle Swarm Optimization Based Artificial Neural Network. In *Springer Nature Book: Metaheuristic and Evolutionary Computation: Algorithms and Applications, under Book Series Studies in Computational Intelligence*; Springer: Singapore, 2020; pp. 283–297. [CrossRef]
41. Minai, A.F.; Malik, H. Metaheuristics Paradigms for Renewable Energy Systems: Advances in Optimization Algorithms. In *Springer Nature Book: Metaheuristic and Evolutionary Computation: Algorithms and Applications, under Book Series Studies in Computational Intelligence*; Springer: Singapore, 2020; pp. 35–61. [CrossRef]
42. Chen, H.; Jiao, S.; Wang, M.; Heidari, A.A.; Zhao, X. Parameters identification of photovoltaic cells and modules using diversification-enriched Harris hawks optimization with chaotic drifts. *J. Clean. Prod.* **2020**, *244*, 118778. [CrossRef]
43. Yu, K.; Qu, B.; Yue, C.; Ge, S.; Chen, X.; Liang, J. A performance-guided JAYA algorithm for parameters identification of photovoltaic cell and module. *Appl. Energy* **2019**, *237*, 241–257. [CrossRef]
44. Yu, K.; Chen, X.; Wang, X.; Wang, Z. Parameters identification of photovoltaic models using self-adaptive teaching-learning-based optimization. *Energy Convers. Manag.* **2017**, *145*, 233–246. [CrossRef]
45. Niu, Q.; Zhang, H.; Li, K. An improved TLBO with elite strategy for parameters identification of PEM fuel cell and solar cell models. *Int. J. Hydrogen Energy* **2014**, *39*, 3837–3854. [CrossRef]